

Dynamic load analysis and design methodology of LCD transfer robot

Jong Hwi Seo¹, Hong Jae Yim^{2,*}, Jae Chul Hwang¹, Yong Won Choi¹ and Dong Il Kim¹

¹Robotics Technology Lab, Mechatronics & Manufacturing Technology Center
SAMSUNG Electronics Co., LTD. Suwon, South Korea

²School of Mechanical and Manufacturing Engineering, Kookmin University SeongBuk-Gu, Seoul, South Korea

(Manuscript Received July 20, 2007; Revised December 28, 2007; Accepted January 16, 2008)

Abstract

The objective of the present study is to develop a design methodology for the large scale heavy duty robot to meet the design requirements of vibration and stress levels in structural components resulting from exposure of system modules to LCD (Liquid Crystal Display) processing environments. Vibrations of the component structures significantly influence the motion accuracy and fatigue damage. To analyze and design a heavy duty robot for LCD transfer, FE and multi-body dynamic simulation techniques have been used. The links of a robot are modeled as flexible bodies using modal coordinates. Nonlinear mechanical properties such as friction, compliance of reducers and bearings were considered in the flexible multi-body dynamics model. Various design proposals are investigated to improve structural design performances by using the dynamic simulation model. Design sensitivity analyses with respect to vibration and stresses are carried out to search an optimal design. An example of an 8G (8th-Generation) LTR (LCD Transfer Robot) is illustrated to demonstrate the proposed methodology. Finally, the results are verified by real experiments including vibration testing.

Keywords: Flexible multibody dynamics; LTR (LCD Transfer Robot); Vibration fatigue

1. Introduction

LCDs are widely used in TV's, computers, mobile phones, etc., because they offer some real advantages over other display technologies. They are thinner and lighter and draw much less power. Recently, the size of raw glass has greatly increased in new generation LCD (Liquid Crystal Display) technology. In order to handle bigger and heavier glasses, it is necessary to develop a large scale LTR (LCD transfer robot) to support various complicated LCD fabrication processes. It will cause many difficult design problems such as vibration, handling accuracy deterioration and high stresses due to heavier dynamic loads, resulting in inaccurate transfer motion and fatigue cracks. Therefore, it is necessary to establish a methodology

for predicting deflections, vibrations, and dynamic stress time histories using virtual computer simulation models. An integrated design simulation method would be useful to validate a baseline design and to propose new improved designs. In this paper an integrated computer simulation methodology is presented to predict deflections, dynamic stresses due to vibrations design, based on the existing FEM and flexible body dynamics technology.

The proposed methodology is applied to the LTR that handles 7G/8G LCD glasses. Vibration analysis is performed and validated with the vibration modal test to identify and to recapture the inherent phenomenon in the system. Some flexible components in the LTR may experience severe vibration to cause fatigue damage due to large dynamic loads. Modal characteristics are used to consider structural flexibility in flexible multi-body dynamic simulations. Tip deflection of the end-effector can be calculated to see

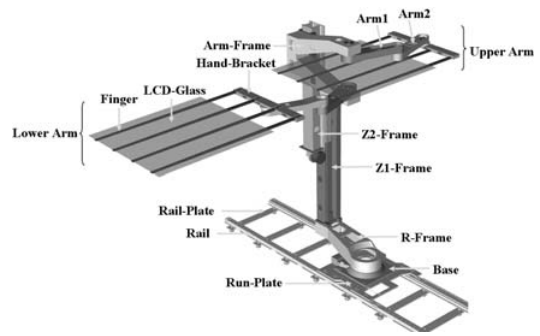
*Corresponding author. Tel.: +82 2 910 4688, Fax.: +82 2 910 4718
E-mail address: hjyim@kookmin.ac.kr
DOI 10.1007/s12206-008-0115-4

if design requirements are met. Dynamic loads and dynamic stress histories can be obtained from the dynamic simulation. Stress levels are investigated at the critical areas to predict if fatigue cracks might occur. If the stress level is not in a safe region, design change should be made based on the computer simulation results and design sensitivity study. Then a prototype LTR is built and tested for design validation. The present paper describes the CAE-based durability analysis that is being implemented and developed at SAMSUNG, to predict fatigue damage corresponding to durability tests. The proposed methodology can be used to develop a new large scale LTR robot in the early design stage.

2. Introduction of LCD-transfer robot

Fig. 1 shows various types of LTRs. Telescope type LTR consists of a base frame, an R-frame, two Z-frames, two articulated arms with slender hands as shown in Fig. 1(a). The frame structures are fabricated with cast iron and aluminium. Hands with slender fingers are made of lightweight composite materials. It also has two arms (upper and lower arms) to handle two glasses simultaneously. The LTR has a cylindrical workspace to transfer glasses for various fabrication processes. For precision control of handling the glasses, static deformation at the tip of the finger must be less than 10 mm. Since the joints which connect the arms and links include bearings and reducers, joint compliance must be considered to predict the static deformation at the tip. Flexibilities of the arm itself are also important to both static and dynamic deformation, because the arm is a kind of cantilever type structure with a large lumped mass at the tip.

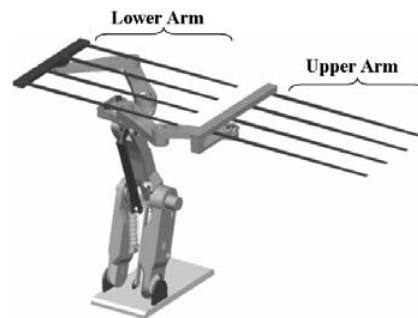
LTR is supposed to repeat millions of cycles to perform LCD fabrication processes in real life. Therefore, it has to pass physical tests to ensure the survivability of the robot system when subjected to static and cyclic loadings. The durability test involves a cyclic loading apparatus that evaluates the durability characteristics of the component structure. Among the many different tests, one of the most critical is the hand motion of stretching out and pulling in with the z-frame’s vertical motion. The critical motion simulates the jerking and twisting impact that an arm support bracket might experience when running with large glasses loaded. The arms and hands are synchronized and moved at a speed of about 4 m/s.



(a) Telescopic type



(b) Gate type



(c) Link type

Fig. 1. LCD Transfer robots (LTR).

Since the LTR repeats millions of cycles of particular loading and unloading with various configurations, it may result in fatigue failure at a critical stress area. In this paper, to predict static and dynamic deformation at the tip of the finger and critical stress levels including vibration of the LTR, flexible multi-body dynamic simulations are presented. Link-frames, arms are modelled as flexible bodies. Static and dynamic deformation is assumed to be very small, therefore, within the linear elastic range. To represent the flexibility, vibration normal modes and static correction modes are obtained from the finite element vibra-

tion and static analysis for each flexible component. To represent the joint compliance, spring and damper force elements are used instead of kinematic joint elements [1].

3. Flexible multi-body dynamics

The main advantage of using modal coordinates in flexible multi-body dynamics is the reduction in the number of generalized coordinates that must be included in the analysis. Two types of modes are used in component mode synthesis for flexible multi-body dynamics [1, 2]. One is a normal mode. The other is a static mode. All used normal modes and static modes must be normalized to have the same magnitude and be orthogonalized to be independent to each other.

3.1 Kinematics of flexible components

A typical flexible component is shown in Fig. 2.

The flexible component i is discretized into a large number of finite elements. The global position of a point p in a flexible part i can be represented as

$$\mathbf{r}_p^i = \mathbf{R}^i + \mathbf{A}^i \bar{\mathbf{u}}^i = \mathbf{R}^i + \mathbf{A}^i (\bar{\mathbf{u}}_o^i + \bar{\mathbf{u}}_f^i) \quad (1)$$

Where \mathbf{R}^i is the global position vector of the X'-Y'-Z' body reference frame, \mathbf{A}^i is the coordinate transformation matrix from the body reference frame to the global inertial frame, $\bar{\mathbf{u}}_o^i$ is the initial position vector of the point p from the body reference frame, and $\bar{\mathbf{u}}_f^i$ is the displacement vector due to deformation. The displacement vector $\bar{\mathbf{u}}_f^i$ can be approximated by a linear combination of deformation modes like Eq. (2).

$$\bar{\mathbf{u}}_f^i = \Psi^i \boldsymbol{\eta}^i = \sum_{j=1}^M \psi_j^i \eta_j^i \quad (2)$$

Where $\Psi^i = \Psi^i(x^i, y^i, z^i) = [\Psi_r^i, \Psi_f^i]$ is a modal matrix and ψ_j^i is the corresponding deformation mode of a flexible part i . $\boldsymbol{\eta}^i = \boldsymbol{\eta}^i(t)$ is a $6N \times 1$ modal vector and η_j^i is modal coordinates, M is the number of modal coordinates. The deformation modes can be normal modes, static modes, or combination of normal and static modes. Used M modes should be linearly independent to each other.

3.2 Flexible multi-body dynamic equations

As shown in Fig. 2, the nodal position vector of a

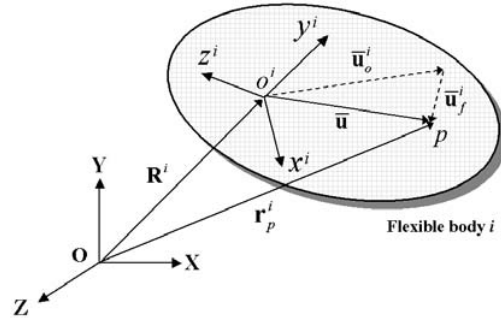


Fig. 2. Global displacement of a point p in a flexible component i .

typical point p in the global reference frame can thus be written as Eq. (3) by using Eq. (2)

$$\begin{aligned} \mathbf{r}_p^i &= \mathbf{R}^i + \mathbf{A}^i \bar{\mathbf{u}}^i = \mathbf{R}^i + \mathbf{A}^i (\bar{\mathbf{u}}_o^i + \Psi_r^i \boldsymbol{\eta}^i) \\ \boldsymbol{\pi}_p^i &= \boldsymbol{\pi}^i + \Psi_r^i \boldsymbol{\eta}^i \end{aligned} \quad (3)$$

Where $\bar{\mathbf{u}}^i = \bar{\mathbf{u}}_o^i + \Psi_r^i \boldsymbol{\eta}^i$ and the rotational displacement $\boldsymbol{\pi}_p^i$ of nodal point p is defined by $\Psi_r^i \boldsymbol{\eta}^i$. The combined set of kinematic and driving constraints of the multi-body dynamic system may be written in the form [3, 4]

$$\Phi(\mathbf{q}, \mathbf{t}) = \mathbf{0} \quad (4)$$

Where the generalized coordinates $\mathbf{q} = [\mathbf{q}_r^T, \mathbf{q}_f^T]^T = [\mathbf{r}^T, \boldsymbol{\pi}^T, \boldsymbol{\eta}^T]^T$, \mathbf{t} is the time, Φ is the constraint equation. Using the Lagrange Multiplier Theorem, variational equations of motion of the multi-body system may be obtained by summing all bodies and constraints in the system as in the matrix form of Eq. (5).

$$\begin{bmatrix} \mathbf{M}^* & \Phi_q^T \\ \Phi_q & \mathbf{0} \end{bmatrix} \begin{bmatrix} \ddot{\mathbf{q}} \\ \boldsymbol{\lambda} \end{bmatrix} = \begin{bmatrix} \mathbf{Q}^* \\ \boldsymbol{\gamma} \end{bmatrix} \quad (5)$$

This is a mixed system of differential-algebraic equations of motion for considering the elastic effect of the mechanical system. To solve mixed differential algebraic equations, many numerical algorithms have been developed [3]. Using Eq. (5), dynamic stress history of a flexible component can be calculated [5].

4. Dynamic modelling of an lcd-transfer robot

The 8G-Telescopic type LTR system shown in Fig.

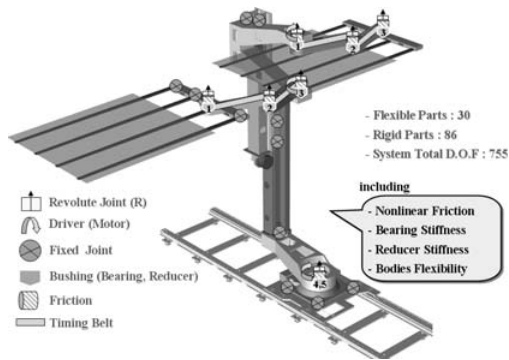
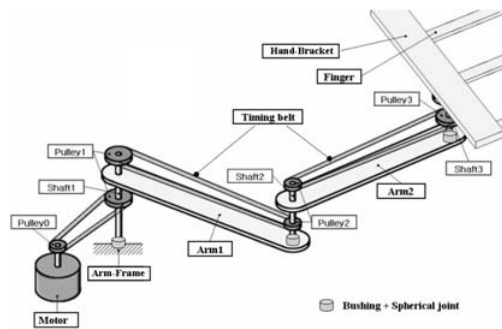
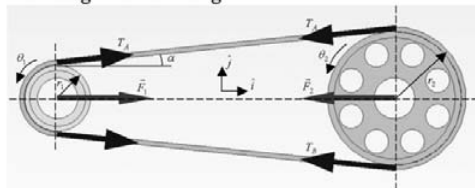


Fig. 3. Flexible multi-body dynamics model for 8G-Telescopic LTR.



* Timing belt modeling



$$T_A = T_0 + k(r_1\theta_1 - r_2\theta_2) + c(r_1\dot{\theta}_1 - r_2\dot{\theta}_2)$$

$$T_B = T_0 - k(r_1\theta_1 - r_2\theta_2) - c(r_1\dot{\theta}_1 - r_2\dot{\theta}_2)$$

$$M_1 = -r_1(T_A - T_B) - f_1(\dot{\theta}_1)_{\text{Nonlinear Friction}}$$

$$M_2 = r_2(T_A - T_B) + f_2(\dot{\theta}_2)_{\text{Nonlinear Friction}}$$

Fig. 4. Dynamic modeling of LTR arm system.

l(a) can be modeled with 86 rigid bodies, 30 flexible bodies, kinematic joints, and force elements [3]. The flexible bodies considered in the multi-body dynamic simulation are named in the Fig. 1(a). Fig. 3 shows the flexible multi-body simulation model for 8G-Telescopic LTR.

For parallel rectilinear motion of the finger and hand-bracket, a timing belt at each arm system is modeled to drive at constant speed ratio. As shown in Fig. 4, to represent the elasticity and damping of the

Table 1. Joint stiffness for bearing and reducers.

No.	Axial Stiffness	Radial Stiffness	Part
1	180 KNm/rad	2570 KNm/rad	Reducer
2	250 KNm/rad	3510 KNm/rad	Reducer
3	67 KNm/rad	1000 KNm/rad	Reducer
4	6745 KNm/rad	43840 KNm/rad	Reducer
5	0	436360 KNm/rad	Bearing



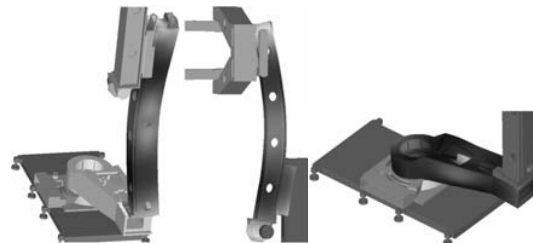
(a) Finger (36)



(b) Arm1 (18)



(c) Arm-Frame (42)



(d) Z1-Frame (24) (e) Z2-Frame (24) (f) R-Frame (36)

Fig. 5. Component modes of flexible bodies (number of modes used for dynamic simulation).

belt, spring and damping forces are approximated to be proportional to displacement and velocity of the belt length change. Even the joint compliances for bearing and reducers are modeled in a similar way with rotational-spring and damper elements. The experimental values from the components' makers are shown in Table 1.

Major components such as arms and link frames are made of cast iron or cast aluminium. Those structural components can be assumed to be linear elastic

during normal operation. However, such a small elastic deformation may cause vibration and repeated dynamic stresses resulting in inaccurate transfer motion and fatigue cracks. Therefore, it is necessary to establish a methodology for predicting the deformation, vibration, and dynamic stress time histories with a virtual computer simulation model.

Component mode synthesis technique [1-4], explained in the previous section, can be used for efficient computer simulation in large rigid body gross motion with small elastic deformation. Since the component mode synthesis method employs modal coordinates to consider the elastic deformation of flexible bodies, it is possible to execute a large multi-body dynamic system analysis more effectively by using a small number of well-selected modes.

Fig. 5 shows the 1st vibration modes of flexible components in the telescopic LTR in Fig. 1(a). Also, Fig. 5 shows a typical component mode and the number of modes used in the mode component synthesis method for the flexible multi-body dynamic analysis.

5. Analysis and design improvement of LTR

5.1. Modal analysis of 8G-telescopic LTR

Since major structural bodies such as arms and link-frames are modelled as flexible bodies, the proper kinematic joints and force elements, fundamental vibration modes of the total LTR system can be investigated. The modes calculated from the vibration analysis can be used for searching for the structural weak point and used for the flexible multi-body

dynamic simulation explained in the previous chapter. Fig. 6 shows the modal deformation from the vibration test of the LTR system. Analytical vibration modes calculated from the dynamic simulation model are compared with the experimental test results for validation. Comparison with the modal test results showed that simulation results correlate well with the test results. From the results of the analytical and experimental modal deformation, we found that the structural weak point was the R-frame. This information was very important to reduce the system vibration, as explained in the following section.

5.2 Vibration analysis and design improvement

Design problems such as tip deflection and fatigue crack can be investigated with a valid simulation model. Among the various process events for LCD glass transfer motion, stretching out and pulling in motions of the hands with glass loaded are the most critical motions to cause severe vibration and high stresses at the supporting bracket structure. Using the proposed flexible multi-body simulation technology, the critical motion is regenerated to investigate how large deflection and stresses occur during the operation. Since we have a valid simulation model, we can investigate various design proposals.

After the prototype robot was developed, undesirable vibration at the measure point was observed when the robot was running onto the guide rail, as shown in Fig. 7. The cause of the vibration was the insufficient stiffness of the R-frame, studying from

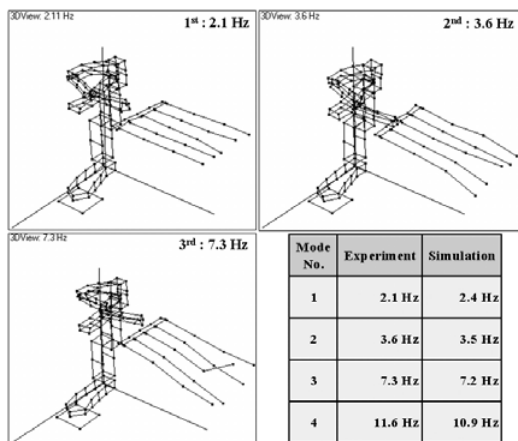


Fig. 6. Vibration modes by experiment and comparison of frequencies

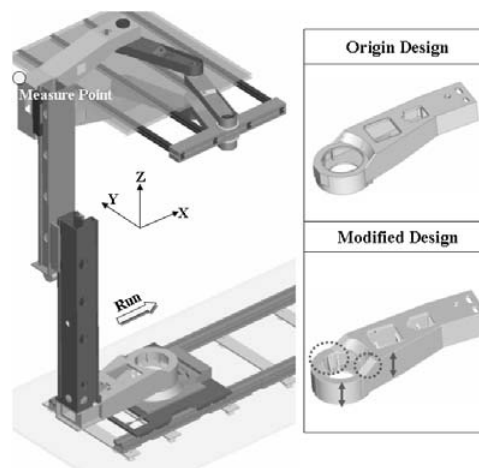


Fig. 7. Design study to reduce the vibration by dynamics simulation.

the analysis of the system modal deformation, as explained in the previous section. In other words, the R-frame at the base of the LTR was known to be a critical component for the vibration.

To increase bending and twisting stiffness, height and width of the beam cross section was enlarged, and ribs were added as explained in the Fig. 7. Even aluminium material is replaced with high strength steel to increase the elastic modulus. To verify the design modification, a dynamic simulation model was used.

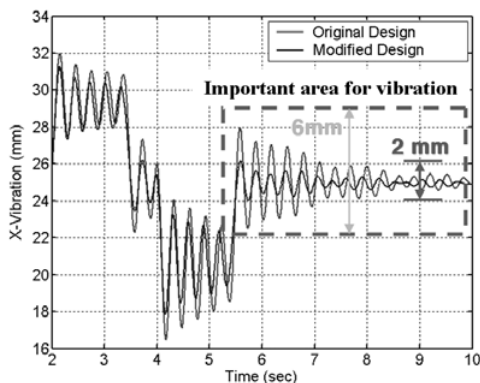


Fig. 8. Comparison of vibration levels between the original and modified design.

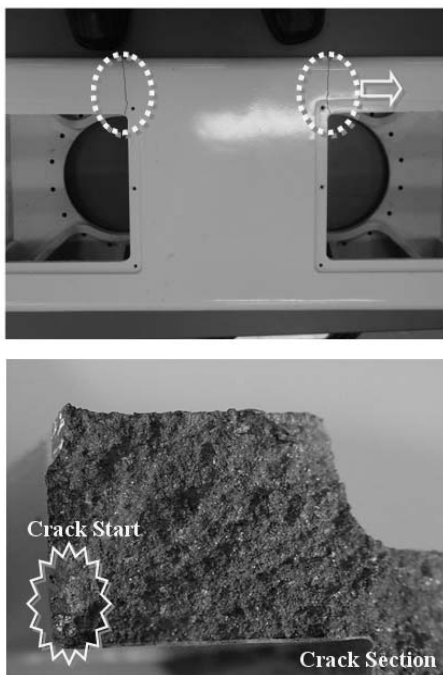


Fig. 9. An example of the crack fatigue.

Fig. 8 shows a comparison of vibration displacements during the simulated motions between the original baseline design and the new improved design. More than 50% reduction of the vibration level is observed during the critical motion period from 5 to 10 seconds even at the prototype test as shown in Fig. 8.

5.3 Stress analysis and design improvement

As the size of raw glass tends to become larger for productivity and manufacturing cost competitiveness, LTR robots need to be faster and bigger to handle the larger and heavier glasses with higher speed. This may result in increased dynamic loads causing fatigue cracks due to dynamic stresses.

Fig. 9 shows an example of the fatigue cracks due to dynamic loads at the supporting arm-frame structure in the 7G-Gate LTR shown in Fig. 1(b). Using the flexible multi-body dynamic simulation, cause and effect for the fatigue crack can be analyzed prior to adoption in an actual spot. To reduce the level of

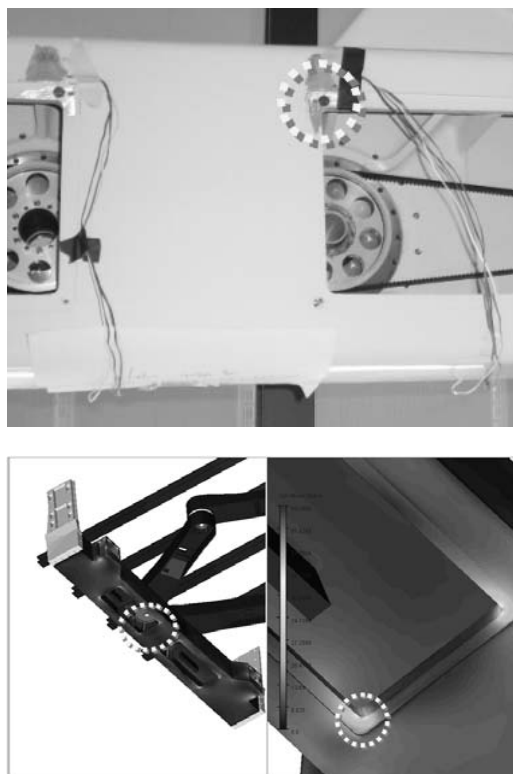


Fig. 10. Strain experiment and dynamic analysis for fatigue life prediction.

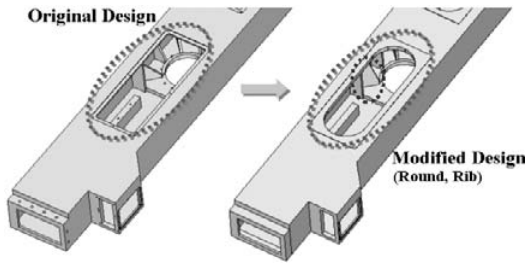


Fig. 11. Design modification for avoiding stress concentration.

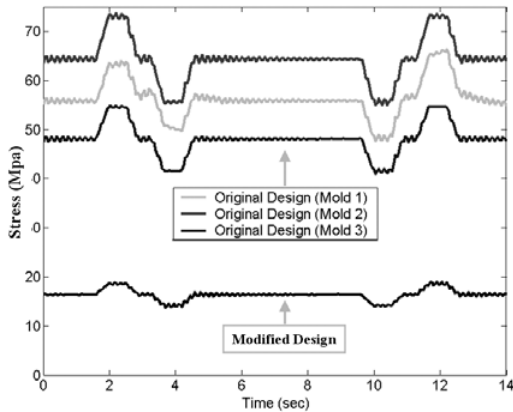


Fig. 12. Stress analysis and design improvement

dynamic stress at the critical area, the shape and thickness of the structure must be redesigned based on the validated simulation model. Experimental tests were executed to validate the accuracy of dynamic stresses predicted in virtual computer simulations, as shown in Fig. 10. And the result was exactly the same as the point of occurrence of the crack.

Fig. 11 shows the design modification. To reduce the stress concentration, the rectangular shape with sharp corners was changed to a round shape, and ribs were changed.

Fig. 12 shows a comparison of maximum dynamic stresses between the modified shape and original shape with different metal thickness. The stress measure point of the part is the dotted circle area in the Fig. 10. This result shows the conclusion that the design was reasonably modified. Practically, the modified design was adopted for the 7G-Gate LTR in the actual spot.

5.4 Handling accuracy and design optimization

If dynamic loads are increased, it might deteriorate

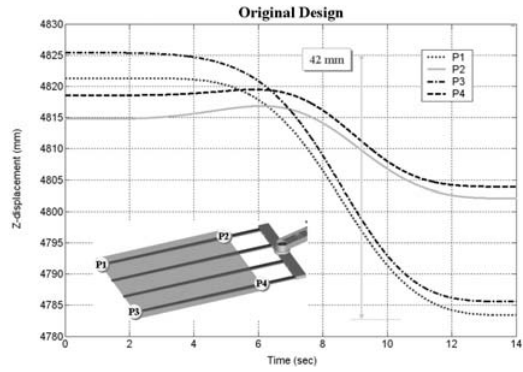


Fig. 13. Vertical deflection of the fingers for baseline design.

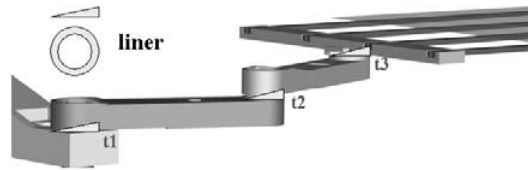


Fig. 14. Robot arm and liner (thin circular plate).

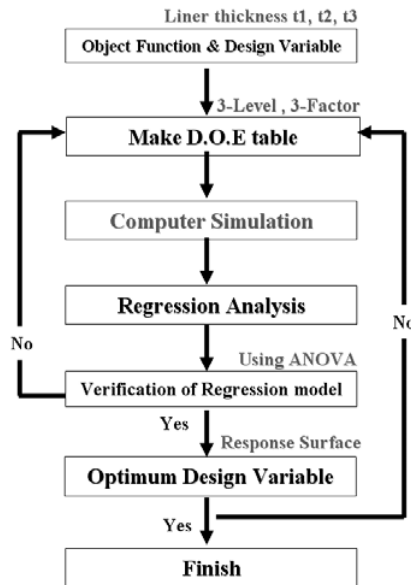


Fig. 15. Process for design variable optimization.

the accuracy of the precision transfer motion due to deflection and deformation of major structural components [6]. Fig. 13 shows the vertical deflections at the tip points of the fingers for the baseline design of the 8G-Telescopic LTR.

The tip deflection of the original design of the LTR was 42 mm. This exceeds the design specification

requirement of 10 mm for the LCD fabrication process, and may be the cause of the collision between cassette and robot hands. The cause of the deflection was that the robot structure was very large and heavy. As a result, the deflection must be reduced and the transfer accuracy improved by using the dynamic simulation and optimized design techniques. To reduce the dynamic deflection, a thin-tapered circular plate, what we called a liner, was used, as shown in Fig. 14.

The combination of the three liners' thickness is very important to reduce the deflection and to optimize the transfer accuracy. So we used dynamic simulations and D.O.E (Design of experiment) for optimization. Fig. 15 shows the proposed simulation methodology which can be used to minimize the deflection at the tip of the finger.

The object function was minimization of the differences of the vertical z-displacement of 4-points in Fig. 13. The used D.O.E table was a central composite design table with 3-levels and 3-factors [7]. Table 2 shows the regression analysis result (ANOVA table).

Through the response surface model calculated from the regression analysis [7], the optimized liner thickness was $t_1=0.50$, $t_2=0.48$, $t_3=0.78$ mm. The simulation results for the optimized variable (liner

Table 2. ANOVA table for optimization.

Factor	S	V	F_0	$F(\sigma)$	P
Regression	175.085 (SSR)	58.362 (MSR)	145.49	22.04	0.002
Residual	4.412 (SSE)	0.401 (MSE)	Coefficient of Determination $R^2 = 97.54\%$		
Sum	179.498 (SST)				

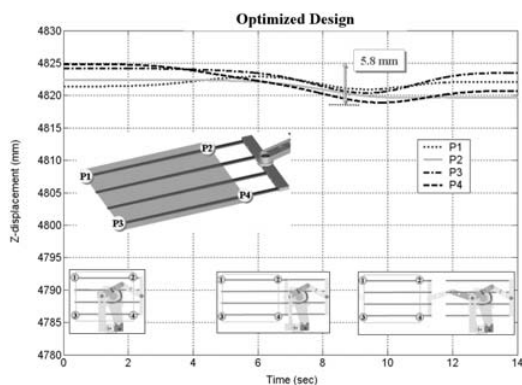


Fig. 16. Optimized design result using dynamic simulation and D.O.E.

thickness) are shown in Fig. 16. The deflection was reduced only to 5.8 mm. But 42 mm deflection occurred in the baseline design as shown in Fig. 13.

An experimental test using the laser tracker was carried out to validate the optimized simulation result. As shown in Fig. 17, the experimental result was about 6.1mm.

The simulation results of dynamic deflection were very similar to the test results. This means that we reinforced the structural stiffness without any additional expense.

6. Conclusions

A computer simulation methodology was presented for vibration and fatigue analysis of the LTR system. Variable amplitude multi-axial loading conditions can be generated to investigate any structural deflection, vibration, and dynamic stress. Flexible bodies were modelled by using component mode synthesis technique. To represent joint compliance and belt flexibility, spring and damper force elements were introduced with proper approximation. To have a valid simulation model, vibration modes of the total LTR system were compared with the modal test results. Comparison of the analysis and test results shows that they correlate well with each other. Deflection of the tip of the end-effector was investigated with the proposed methodology. To reduce the tip deflection, a better design can be developed with the simulation model. Fatigue crack failure related to the dynamic stress can be predicted with the baseline design. To prevent fatigue failure at a critical area, stresses were reduced by changing the structural design. The results of the virtual durability assessment were quite good, and showed good correlation with the areas of failure

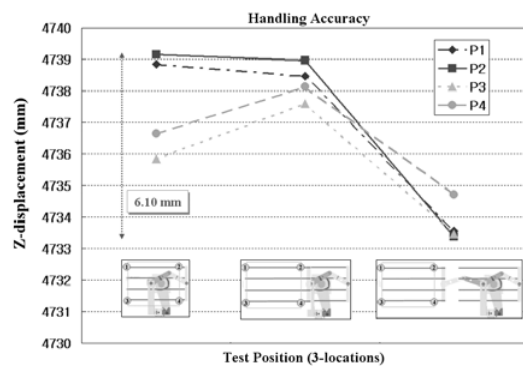


Fig. 17. Test result for vertical deflection

on the test. The value of being able to predict service lives based on results obtained exclusively in the virtual domain is obvious. The proposed methodology can be used to develop another type of LTR system.

Acknowledgment

This work was partly supported by the Seoul Research & Business Development Program (Grant No. 10583) and the research program 2007 of Kookmin University in Korea.

References

- [1] A. A. Shabana, Dynamics of multibody systems 2nd Edition, Cambridge University Press, (1998).
- [2] S. C. Wu, E. J. Haug and S. S. Kim, A variational approach to dynamics of flexible multibody systems, CCAD Technical Report 86, University of Iowa, (1986), 15.
- [3] Kim S. S. and Haug E. J., Selection of deformation modes for flexible multibody dynamics, *Mechanics of structures and machines*. 18 (4) (1990) 565-586.
- [4] S. S. Shin, W. S. You and J. Tang, Effect of mode selection, scaling, and orthogonalization on the Dynamic analysis of flexible multibody systems. *Mechanics of Structures and machines*. 21 (4) (1993), 507-527.
- [5] J. H. Ryu, H. Kim and H. J. Yim, An efficient and accurate dynamic stress computation by flexible multibody dynamic system simulation and reanalysis, *Journal of Mechanical Science and Technology*, 11 (4) (1997) 386-396.
- [6] J. C. Hwang, K. S. Byun and Y. W. Choi, "Improvement of the path accuracy of the 7th generation LCD glass transfer robot, International Conference on Mechatronics and Information Technology, Chongqing, China, (2005).
- [7] S. H. Park, Modern Design of Experiments, Minyeongsa, (1995).